Spatially Modulated Tunnel Magnetoresistance on the Nanoscale

Hirofumi Oka, Kun Tao, Sebastian Wedekind, Guillemin Rodary,* Valeri S. Stepanyuk,† Dirk Sander,‡ and Jürgen Kirschner

Max-Planck-Institut für Mikrostrukturphysik, Weinberg 2, D-06120 Halle/Saale, Germany

(Received 15 July 2011; published 25 October 2011)

We investigate the local tunnel magnetoresistance (TMR) effect within a single Co nanoisland using spin-polarized scanning tunneling microscopy. We observe a clear spatial modulation of the TMR ratio with an amplitude of ~20% and a spacing of ~1.3 nm between maxima and minima around the Fermi level. This result can be ascribed to a spatially modulated spin polarization within the Co island due to spin-dependent quantum interference. Our combined experimental and theoretical study reveals that spin-dependent electron confinement affects all transport properties such as differential conductance, conductance, and TMR. We demonstrate that the TMR within a nanostructured magnetic tunnel junction can be controlled on a length scale of 1 nm through spin-dependent quantum interference.

DOI: 10.1103/PhysRevLett.107.187201 PACS numbers: 75.75.Lf, 68.37.Ef, 73.40.Gk, 75.76.+j

One of the hallmarks of quantum mechanics is the concept of tunneling. Electrons can tunnel from one electrode through a barrier into another electrode. This process is spin-dependent. In the case of magnetic electrodes, the magnitude of the tunneling current depends, among other factors, on the relative magnetization directions of both electrodes. This dependence is known as the tunnel magnetoresistance (TMR) effect [1–3]. It is the basis of the functionality of read heads used in current technology hard disk drives and in magnetic random access memory applications. Thus, exploring novel venues towards tuning the TMR in nanostructures is decisive to develop integrated spintronic devices with reduced dimensions.

In this Letter, we demonstrate local control of the TMR on a nanometer scale by exploiting spin-dependent quantum interference within a single Co nanostructure [4,5]. We use spin-polarized scanning tunneling microscopy (STM) [6] to image and to quantify the TMR ratio on an individual Co nanoisland. We find a clear spatial modulation of the TMR with an amplitude of ~20% around the Fermi level. The TMR modulation pattern depends on island size and energy. This demonstrates that spin-polarized tunneling channels are tunable on the nm scale by quantum interference, opening a new venue towards local control of the TMR.

We carried out spin-polarized STM measurements using an ultrahigh vacuum STM at a low temperature of 8 K and under magnetic fields of up to 4 T. The magnetic field is applied perpendicular to the sample surface, which is the easy magnetization direction of Co islands on Cu(111) [7,8]. A small amount of Co [~ 0.4 monolayer (ML)] was deposited onto an atomically clean Cu(111) substrate at room temperature. STM tips to detect magnetic signals were prepared by deposition of magnetic materials on flashed W tips. In this study, tips covered with a Cr film and an underlayer of Co [Cr(40 ML)/Co(40 ML)/W tips] were used.

Figure 1(a) shows the tunnel current as a function of bias voltage [$I(V)$ curves] at different magnetic fields. The $I(V)$ curves are measured at the same point at the center of the nm-small Co island [inset in Fig. 1(a)], to avoid any contributions of position-dependent electronic properties to the tunnel current [4,5,9,10]. The $I(V)$ curves recorded at −1.1 T (blue) and at 0.0 T (dashed black) are almost identical. However, the second curve obtained at −1.1 T (red), after a field sweep to +4.0 T and coming back to −1.1 T, shows a different behavior, e.g., at −0.27 V. This difference is ascribed to the TMR effect. The tunnel current depends on the relative orientation of the tip and island magnetizations [1–3], and this orientation is different for these two measurements. This becomes obvious from the hysteresis curve of Fig. 1(b). Figure 1(b) shows a plot of the tunnel current as a function of the magnetic field B at a bias voltage of −0.27 V, revealing the hysteretic behavior of the $I(B)$ signal. We identify parallel (P) and antiparallel (AP) alignments of the magnetization directions of the tip and the Co island, as illustrated in Fig. 1(b) [11]. Thus, we conclude that the sharp change of the tunnel current at ±0.5 and ±1.3 T is caused by a transition between AP and P states [8]. As we know the tunnel current and the gap voltage, we extract the TMR and the TMR ratio [12,13], defined as

$$\frac{R_{\mathrm{AP}} - R_{\mathrm{P}}}{R_{\mathrm{P}}} = \frac{I_{\mathrm{P}} - I_{\mathrm{AP}}}{I_{\mathrm{AP}}}, \tag{1}$$

where I_{AP} and I_{P} are the tunnel currents and R_{AP} and R_{P} are the tunnel resistances in the AP and P states, respectively. The right scales of Fig. 1(b) reveal that the tunnel resistance varies between 290 and 190 MΩ, and we calculate a maximum positive TMR ratio of ~50%.

The TMR depends on the electronic properties of both electrodes [14,15] (here, the Co island and the tip), and a pronounced energy dependence is expected in view of the distinct spectral features of the spin-resolved electronic

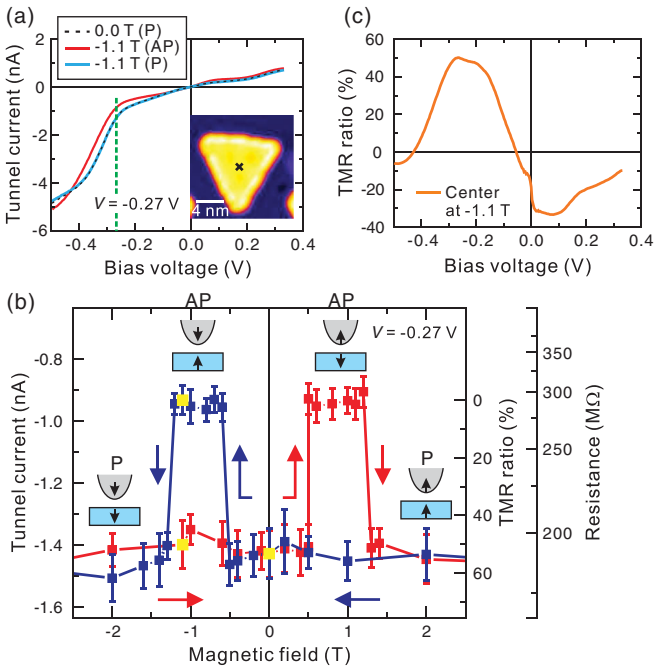

FIG. 1 (color). The tunnel current, its magnetization dependence, and the TMR spectrum. (a) $I(V)$ curves measured at the center of the Co island, shown in the inset at different magnetic fields ($V_{\mathrm{stab}} = +0.5$ V, $I_{\mathrm{stab}} = 1.0$ nA). The dashed line at -0.27 V gives the bias voltage of the measurement of the hysteresis curve in (b). The inset shows a constant-current STM image of the Co island on Cu(111) ($V_S = -0.1$ V, $I = 1.0$ nA). (b) Hysteresis loop of the tunnel current measured at the center of the Co island. The red and blue sections of the hysteresis loop correspond to upward and downward sweeps of the magnetic field, respectively. Yellow dots in the loop indicate measurement conditions of the $I(V)$ curves shown in (a). Schematics indicate the magnetization orientations of the Co island and the magnetic tip. (c) TMR spectrum measured at the center of the Co island, which is obtained from the two $I(V)$ curves at -1.1 T in (a) using Eq. (1).

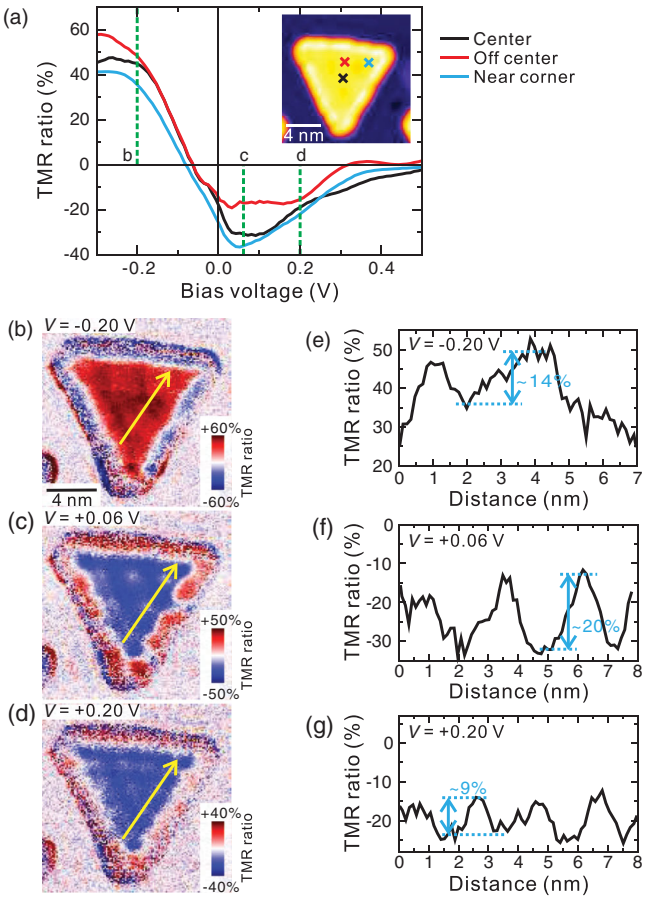

FIG. 2 (color). Spatial modulation of TMR within a single Co island and its energy dependence. (a) TMR spectra as a function of bias voltage V taken at three different positions on the Co island of Fig. 1, shown in the inset. Corresponding positions are indicated by crosses. Each TMR spectrum is obtained from two $I(V)$ curves measured at P and AP magnetization configurations at -1.1 T, using Eq. (1). (b)–(d) Maps of the TMR ratio obtained at the indicated voltages ($V_{\mathrm{stab}} = +0.5$ V, $I_{\mathrm{stab}} = 1.0$ nA, -1.1 T). The selected voltages are indicated by green dashed lines in (a). (e)–(g) Line profiles, averaged over 6 adjacent lines for an improved signal-to-noise ratio, of the TMR ratio images along the yellow arrows in (b)–(d).

density of states of the Co island [5]. This spectral dependence of the TMR ratio is plotted in Fig. 1(c), where the tunnel current I in P and AP configurations has been measured at different bias voltages. Below $V = -0.05$ V, the TMR ratio is positive and reaches its maximum of $\sim$50% around -0.27 V. Above -0.05 V, it changes sign and decreases to $\sim -30\%$ around $+0.08$ V.

As a next step, we exploit the spatial resolution of the STM to investigate the position dependence of the TMR within a single Co island. We measure TMR spectra at three different positions 1–2 nm apart within the same Co island [Fig. 2(a)]. All spectra show a similar bias-voltage dependence, as discussed above; however, we observe distinct differences in the magnitude of the TMR ratio. We map the spatial variation of the TMR ratio within the same Co island at fixed bias voltage and show the result in Figs. 2(b)–2(d) [11]. These images reveal a pronounced variation of the TMR ratio within the Co nanostructure.

At $V = +0.06$ V [Fig. 2(c)], the TMR map reveals a positive TMR ratio near the edge of the Co island, whereas it is negative and spatially modulated in the center region. This observation is explained by the spin-resolved electronic density of states of Co islands on Cu(111). Around the Fermi energy ($V = +0.06$ V), the rim of a Co island exhibits a negative spin polarization originating from a minority d state [9], and the inner part of the island shows a positive spin polarization originating from the majority s-p surface state [4,16]. In addition, the spin polarization is spatially modulated within a Co island due to spin-dependent quantum interference [5]. The modulation pattern found in the TMR ratio map [Fig. 2(c)] is similar to that of a dI/dV asymmetry map, which qualitatively

corresponds to a map of the spin polarization [5,11]. Our data indicate that a reduced spin polarization induces a reduced TMR ratio. This result demonstrates that TMR within a single Co island is spatially modulated due to spin-dependent quantum interference.

We have shown earlier that the spatial modulation of the spin polarization changes with energy [5]. Consequently, one might expect to observe similar changes in the modulation pattern of the TMR. In Figs. 2(b)–2(d), we display TMR ratio maps for different energies (bias voltages), which exhibit clear changes of the spatial modulation patterns. To quantitatively analyze our data, we take line profiles through the TMR images. All profiles [Figs. 2(e)–2(g)] show a clear corrugation identifying the spatial modulation of the TMR. We find that, at +0.06 V [Fig. 2(f)], the TMR ratio within the Co island is modulated with an amplitude of ~20% and a spacing of ~1.3 nm between maxima and minima. At +0.20 V [Fig. 2(g)], we find a modulation amplitude of ~9% with a spacing between maxima and minima of ~1.0 nm. The examples reveal that the TMR ratio modulation shows a shorter periodicity with increasing bias voltage.

To understand the energy dependence of the TMR ratio shown in Fig. 1(c), we calculate spin-dependent transport properties of a model system, schematically depicted in the inset of Fig. 3(a), with the SMEAGOL code [11,17–19]. The calculated TMR ratio is presented in Fig. 3(a). Comparing the calculations with our experimental results of Fig. 1(c) [20], we find a good qualitative agreement. From this, we conclude that our calculations are well-suited to describe the spin-dependent transport properties of our system and we apply our theory to discuss the electronic origin of the energy dependence of the TMR ratio. To explore the impact of the exact atomic configuration of the tip on the transport properties, we also calculated the transmission for a tip apex which consists of a Cr cluster. We obtain qualitatively the same results [11].

A decisive property in the calculation of the tunnel current is the transmission coefficient. Its energy integral gives the tunnel current, where the energy interval is given by the bias voltage. We show the transmission coefficient as a function of energy at different bias voltages for P and AP configurations for spin-up and spin-down channels in Fig. 3(b). We find peaks (labels 1 and 2) in the transmission curves, which govern the amplitude of the tunnel current and consequently the amplitude and the sign of the TMR ratio.

At $V = 0.0$ V, the transmission coefficient at the Fermi energy in the P configuration is $0.062G_0$ for the spin-up channel and $0.046G_0$ for the spin-down channel, where $G_0 = 2e^2/h$, with e being the electronic charge and h the Planck constant. The transmission at the Fermi energy in AP is $0.099G_0$ ($0.019G_0$) for the spin-up (spin-down) channel. The sum of them in AP ($0.118G_0$) is larger than the one in P ($0.108G_0$), resulting in a negative TMR ratio

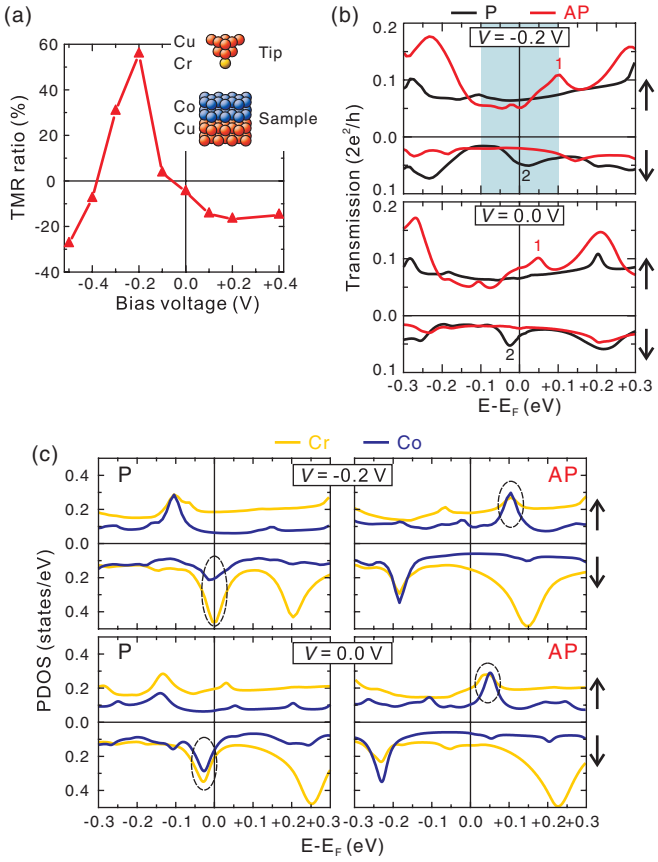

FIG. 3 (color). Energy dependence of spin-dependent transport properties. (a) Calculated energy-dependent TMR ratio. The inset shows the model of the tip and sample used in our calculations. (b) Spin-resolved transmission coefficient as a function of energy for both P and AP configurations at different bias voltages. The colored areas denote the bias window within which the transmission function is integrated to obtain the current. (c) s-p PDOS of a Cr atom at a tip apex and a Co atom under the apex in P and AP configurations at bias voltages of $V = -0.2$ V (upper panel) and $V = 0.0$ V (lower panel). Up and down arrows indicate spin-up and spin-down channels, respectively.

[Fig. 3(a)]. The transmission peak 1 mainly causes this larger transmission coefficient in AP.

The transmission coefficient is linked to the transition between electronic states of the Cr tip and the Co island. Thus, to appreciate the electronic origin of a large transmission coefficient, we explore the projected density of states (PDOS) of a Cr atom at the tip apex and a Co atom just under the apex. In general, d states are more localized and decrease sharply into the vacuum, as compared to s-p states, which extend further into the vacuum region. At larger tip-sample separations of the order of 0.5 nm, the interaction between d states of the tip and d states of the sample occurs indirectly via an interaction of s-p states [21–23]. Therefore, at the typical tip-sample distance of 0.5 nm in the STM experiment, the effect of d states on the transmission is small and s-p states give a dominant contribution [23], and we focus on these states. We plot the

PDOS on s-p orbitals of the Cr atom (tip) and the Co atom (island) in Fig. 3(c). At $V = 0.0$ V [lower panel in Fig. 3(c)], in the spin-up channel for the AP state, we find peaks for both PDOSs, Cr and Co, near $+0.1$ eV, where the transmission peak 1 is found. Therefore, we identify the electronic origin of the large transmission peak 1 as being caused by the transition of the spin-up s-p states between the Cr tip and the Co island.

The application of the gap voltage (external bias) corresponds to a relative shift of the position of the PDOSs. Moreover, the intensity of the PDOS also changes because different atomic orbitals respond differently to the electric field induced by the external bias, and this results in a nontrivial change of the transmission coefficient. This is the most important aspect which needs to be considered to understand the energy dependence of spin-dependent transport properties.

The upper panel in Fig. 3(c) reveals that, with a negative bias of -0.2 V, in the spin-down channel for the P state, the Co s-p states shift up in energy towards the Fermi energy and broaden and the Cr s-p states also shift up and increase in amplitude. This gives rise to the broad transmission peak 2 in Fig. 3(b), which is responsible for the large positive TMR ratio shown in Fig. 3(a) at -0.2 V.

In conclusion, our combined experimental and theoretical study reveals that spin-dependent electron confinement affects all transport properties such as differential conductance, conductance, and TMR. We quantify the resulting spatial modulation of the TMR and its spectral dependence and offer an explanation on the electronic level. We demonstrate that the TMR within a nanostructured magnetic tunnel junction can be controlled on a length scale of 1 nm through spin-dependent quantum interference by tuning the energy, the TMR measurement position, and the size of the magnetic nanostructure.

Partial support by Deutsche Forschungsgemeinschaft Grant No. SFB762 is gratefully acknowledged.

*Present address: Laboratoire de Photonique et de Nanostructures, CNRS UPR20, Route de Nozay, 91460 Marcoussis, France.

†stepanyu@mpi-halle.de

‡sander@mpi-halle.de

[1] M. Julliere, Phys. Lett. A **54**, 225 (1975).

[2] T. Miyazaki and N. Tezuka, J. Magn. Magn. Mater. **139**, L231 (1995).

[3] J. S. Moodera, L. R. Kinder, T. M. Wong, and R. Meservey, Phys. Rev. Lett. **74**, 3273 (1995).

[4] L. Niebergall, V. S. Stepanyuk, J. Berakdar, and P. Bruno, Phys. Rev. Lett. **96**, 127204 (2006).

[5] H. Oka, P. A. Ignatiev, S. Wedekind, G. Rodary, L. Niebergall, V. S. Stepanyuk, D. Sander, and J. Kirschner, Science **327**, 843 (2010).

[6] M. Bode, Rep. Prog. Phys. **66**, 523 (2003).

[7] O. Pietzsch, A. Kubetzka, M. Bode, and R. Wiesendanger, Phys. Rev. Lett. **92**, 57202 (2004).

[8] G. Rodary, S. Wedekind, D. Sander, and J. Kirschner, Jpn. J. Appl. Phys. **47**, 9013 (2008).

[9] O. Pietzsch, S. Okatov, A. Kubetzka, M. Bode, S. Heinze, A. Lichtenstein, and R. Wiesendanger, Phys. Rev. Lett. **96**, 237203 (2006).

[10] M. V. Rastei, B. Heinrich, L. Limot, P. A. Ignatiev, V. S. Stepanyuk, P. Bruno, and J. P. Bucher, Phys. Rev. Lett. **99**, 246102 (2007).

[11] See Supplemental Material at http://link.aps.org/supplemental/10.1103/PhysRevLett.107.187201 for additional data and details on measurement techniques and theoretical calculations.

[12] S. S. P. Parkin, C. Kaiser, A. Panchula, P. M. Rice, B. Hughes, M. Samant, and S. H. Yang, Nature Mater. **3**, 862 (2004).

[13] S. Yuasa, T. Nagahama, A. Fukushima, Y. Suzuki, and K. Ando, Nature Mater. **3**, 868 (2004).

[14] J. M. De Teresa, A. Barthélémy, A. Fert, J. P. Contour, F. Montaigne, and P. Seneor, Science **286**, 507 (1999).

[15] E. Y. Tsymbal, O. N. Mryasov, and P. R. LeClair, J. Phys. Condens. Matter **15**, R109 (2003).

[16] L. Diekhöner, M. A. Schneider, A. N. Baranov, V. S. Stepanyuk, P. Bruno, and K. Kern, Phys. Rev. Lett. **90**, 236801 (2003).

[17] A. R. Rocha, V. M. García-Suárez, S. Bailey, C. Lambert, J. Ferrer, and S. Sanvito, Phys. Rev. B **73**, 085414 (2006).

[18] A. R. Rocha, V. M. García-Suárez, S. Bailey, C. Lambert, J. Ferrer, and S. Sanvito, Nature Mater. **4**, 335 (2005).

[19] I. Rungger and S. Sanvito, Phys. Rev. B **78**, 035407 (2008).

[20] The position of occupied minority Co d_{z^2} states calculated by siesta code is about 0.1 eV higher than Korringa-Kohn-Rostoker results [5] and 0.2 eV higher than the experimental results [10]. Therefore, we shift the Fermi level to the higher energy by 0.2 eV.

[21] C. Zener, Phys. Rev. **81**, 440 (1951).

[22] C. Zener, Phys. Rev. **82**, 403 (1951).

[23] K. Tao, V. S. Stepanyuk, W. Hergert, I. Rungger, S. Sanvito, and P. Bruno, Phys. Rev. Lett. **103**, 057202 (2009).